

Enhanced Kerr nonlinearity for self-action via atomic coherence in a four-level atomic system

Tao Hong, Michael Wong Jack, Makoto Yamashita and Takaaki Mukai

NTT Basic Research Laboratories, NTT Corporation,

3-1, Morinosato-Wakamiya, Atsugi-shi, Kanagawa 243-0198, Japan

Abstract

Enhancement of optical Kerr nonlinearity for self-action by electro-magnetically induced transparency in a four-level atomic system including dephasing between the ground states is studied in detail by solving the density matrix equations for the atomic levels. We discern three major contributions, from energy shifts of the ground states induced by the probe light, to the third-order susceptibility in the four-level system. In this four-level system with the frequency-degenerate probes, quantum interference amongst the three contributions can, not only enhance the third-order susceptibility more effectively than in the three-level system with the same characteristic parameters, but also make the ratio between its real and imaginary part controllable. Due to dephasing between the two ground states and constructive quantum interference, the most effective enhancement generally occurs at an offset that is determined by the atomic transition frequency difference and the coupling Rabi frequency.

PACS numbers: 42.50.Gy; 32.80.Qk; 42.65.-k

I. INTRODUCTION

The weak nonlinear response of even the best materials has been a dominant limitation in experimental research on quantum nonlinear optics for many years. A number of theoretical proposals, including the creation of a two-photon bound state [1] and few-photon quantum solitons [2], have not yet been experimentally realized due to the lack of large-Kerr-nonlinear materials. However, recent research surrounding electro-magnetically induced transparency (EIT) [3], which uses atomic coherence to reduce absorption, has opened up a completely new route to achieving large optical nonlinearity [4, 5, 6, 7, 8]. An EIT medium generally possesses two important features: vanishing resonant absorption and, simultaneously, a refractive index curve with a very steep gradient [3]. These two features can significantly enhance the nonlinear interaction strength in multi-level atomic systems. In addition, the latter can also significantly reduce the group velocity of a probe light pulse and therefore greatly increase the effective interaction time of the pulse with the medium [7, 10]. These features may therefore enable one to use an EIT medium to achieve nonlinear optical processes at very low light intensities, or even at energies of a few photons per atomic cross section [7, 8]. Recently, many EIT-enhanced nonlinear phenomena have been observed in experiments, including the Kerr effect [5, 11, 12, 13]. Of particular interest to the present work, Wang et al. have measured the Kerr nonlinear coefficient for self-phase modulation using a three-level system in Rubidium vapor and demonstrated that the nonlinear coefficient is indeed enhanced by EIT [14].

In addition to the scheme involving three atomic levels, a four-level system is also a candidate for the enhancement of the Kerr nonlinearity for self-phase modulation [15]. It is not clear at present which, the three-level system or the four-level system, provides the most advantages for the enhancement of Kerr nonlinearity for self-action (self-phase modulation, two-photon absorption) for very weak light. Or alternatively, because a four-level system in some sense contains a three-level subsystem, how does the presence of the fourth level effect the enhancement of the nonlinearity? In addition, the four-level system considered in Ref. [15] did not include the dephasing between the two ground states. How does the dephasing, which is present in all realistic systems, alter the effective enhancement of the nonlinearity? In order to answer these two questions, in this paper we analyze a four-level system with dephasing between the ground states. First, in section II we quantitatively compare a four-

level EIT scheme for self-action with the corresponding three-level scheme. We discern that there are three major contributions, due to energy shifts of the ground states induced by the probe field, to the third-order susceptibility in the four-level system, and we find that quantum interference amongst the three contributions can, not only enhance the third-order susceptibility more effectively in the four-level system than in the three-level system, but also make the ratio between its real and imaginary part controllable. Next, in section III we analyze the detailed behavior of the most effectively enhanced nonlinearity in the four-level system. As a result we find that in general, the most effective enhancement does not occur exactly at the center of the transparency window due to quantum interference and a finite dephasing rate. On the contrary, it occurs at an offset that is determined by the atomic transition frequency difference and the coupling Rabi frequency.

II. THEORETICAL MODEL

We consider the interaction of two light fields, a coupling field and a degenerate probe field, with a gas of atoms, as shown in Fig. 1. We assume the atoms can be described by the four-level atomic scheme. Consider the case when most atoms are in the ground state $|1\rangle$, by applying a strong coupling light between the states $|2\rangle$ and $|3\rangle$, we can dramatically reduce the resonant absorption for the weak probe light on the transitions $|1\rangle \leftrightarrow |3\rangle$ and $|2\rangle \leftrightarrow |4\rangle$ (see Fig. 1). Under the rotating wave approximation, this four-level system can be described by the following density matrix equations in a frame rotating at frequency ω_p [16]:

$$\dot{\rho}_{11} = \gamma_{31}\rho_{33} + \frac{i}{2}[\Omega_{13}\rho_{31} - \Omega_{13}^*\rho_{13}] \quad (1)$$

$$\dot{\rho}_{21} = [i(\Delta_{13} - \Delta_{23}) - \gamma_{21}]\rho_{21} + \frac{i}{2}[\Omega_{23}\rho_{31} + \Omega_{24}\rho_{41} - \Omega_{13}^*\rho_{23}] \quad (2)$$

$$\dot{\rho}_{31} = [i\Delta_{13} - \frac{1}{2}(\gamma_{31} + \gamma_{32})]\rho_{31} + \frac{i}{2}[\Omega_{13}^*(\rho_{11} - \rho_{33}) + \Omega_{23}^*\rho_{21}] \quad (3)$$

$$\dot{\rho}_{41} = [i(\Delta_{24} + \Delta_{13} - \Delta_{23}) - \frac{1}{2}(\gamma_{40} + \gamma_{42})]\rho_{41} + \frac{i}{2}[\Omega_{24}^*\rho_{21} - \Omega_{13}^*\rho_{43}] \quad (4)$$

$$\dot{\rho}_{22} = \gamma_{32}\rho_{33} + \gamma_{42}\rho_{44} + \frac{i}{2}[\Omega_{23}\rho_{32} + \Omega_{24}\rho_{42} - \Omega_{23}^*\rho_{23} - \Omega_{24}^*\rho_{24}] \quad (5)$$

$$\dot{\rho}_{32} = [i\Delta_{23} - \frac{1}{2}(\gamma_{31} + \gamma_{32})]\rho_{32} + \frac{i}{2}[\Omega_{13}^*\rho_{12} + \Omega_{23}^*(\rho_{22} - \rho_{33}) - \Omega_{24}^*\rho_{34}] \quad (6)$$

$$\dot{\rho}_{42} = [i\Delta_{24} - \frac{1}{2}(\gamma_{40} + \gamma_{42})]\rho_{42} + \frac{i}{2}[\Omega_{24}^*(\rho_{22} - \rho_{44}) - \Omega_{23}^*\rho_{43}] \quad (7)$$

$$\dot{\rho}_{33} = -(\gamma_{31} + \gamma_{32})\rho_{33} + \frac{i}{2}[\Omega_{13}^*\rho_{13} + \Omega_{23}^*\rho_{23} - \Omega_{13}\rho_{31} - \Omega_{23}\rho_{32}] \quad (8)$$

$$\dot{\rho}_{43} = [i(\Delta_{24} - \Delta_{23}) - \frac{1}{2}(\gamma_{31} + \gamma_{32} + \gamma_{40} + \gamma_{42})]\rho_{43} + \frac{i}{2}[\Omega_{24}^*\rho_{23} - \Omega_{13}\rho_{41} - \Omega_{23}\rho_{42}] \quad (9)$$

$$\dot{\rho}_{44} = -(\gamma_{40} + \gamma_{42})\rho_{44} + \frac{i}{2}[\Omega_{24}^*\rho_{24} - \Omega_{24}\rho_{42}] \quad (10)$$

where ρ_{ij} is the density matrix element, $\Omega_{13} = \mu_{13}E_{p0}/\hbar$ and $\Omega_{24} = \mu_{24}E_{p0}/\hbar$ are complex Rabi frequencies for the probe light field amplitude E_{p0} , and $\Omega_{23} = \mu_{23}E_{c0}/\hbar$ is the complex Rabi frequency for the coupling light with electric field amplitude E_{c0} , where μ_{13} and μ_{24} are electric dipole matrix elements. γ_{21} is the dephasing rate between the ground states $|1\rangle$ and $|2\rangle$ (This was not included in Ref. [15]). The detuning angular frequencies are given by $\Delta_{13} = \omega_p - \omega_{31}$, $\Delta_{23} = \omega_c - \omega_{32}$, $\Delta_{24} = \omega_p - \omega_{42}$, where ω_{31} , ω_{32} , ω_{42} are the atomic transition frequencies. Additionally, we assume the probe light is very weak, and the coupling light is on resonance ($\Delta_{23} = 0$). Under this assumption, there is a much larger probability of the atoms being in the ground state $|1\rangle$ than in other states, i.e., $\rho_{11} \approx 1$. Because the evolution of the atoms is very fast and the light is normally approximated as a continuous wave, we can consider the atoms to be in steady states. For simplicity of discussion, we assume uniform decay rates and uniform electric dipole matrix elements, i.e., $\gamma_{31} = \gamma_{32} = \gamma_{40} = \gamma_{42} = \gamma$ and $\mu_{13} = \mu_{24} = \mu$.

Due to the degeneracy of the probe frequency, the polarization induced by the probe field is a superposition of the two off-diagonal density matrix elements,

$$P = n(\mu_{13}\rho_{31} + \mu_{24}\rho_{42})e^{-i\omega_p t} + c.c. \quad (11)$$

where n is the atom density. It is worth noting that this linear superposition gives rise to quantum interference between the two off-diagonal density matrix elements, because the two quantities are complex functions and there is coherence among the atomic states. For example, if the transition amplitudes ρ_{31} and ρ_{42} are in phase, an effective two-photon transition will be enhanced; on the other hand, if the two amplitudes are out of phase, then a photon emitted on one transition will be absorbed on the other and the effective two-photon transition will be suppressed. It is evident that there is no interference between the two off-diagonal density matrix elements in the four-level system with frequency-non-degenerate probes [6]. Thus this superposition of the two off-diagonal density matrix elements is a unique feature of the four-level system with one frequency-degenerate probe. Because the probe field is monochromatic, the corresponding susceptibility has the simple form,

$$\varepsilon_0 (\chi^{(1)}(E_{c0})E_{p0} + \chi^{(NL)}(E_{c0}, E_{p0})E_{p0}^3) = 2n(\mu_{13}\rho_{31} + \mu_{24}\rho_{42}) \quad (12)$$

where $\chi^{(1)}$ is the linear susceptibility and $\chi^{(NL)}$ the nonlinear susceptibility. When $E_{p0} \rightarrow 0$, $\chi^{(NL)}$ corresponds to the third-order susceptibility $\chi^{(3)}$. The real part of $\chi^{(3)}$ is proportional to the Kerr refractive index and the imaginary part of $\chi^{(3)}$ to the two-photon absorption coefficient. Here, $\chi^{(2)}$ does not exist because of the symmetry of the atomic medium. Although the occupation probabilities of atoms on both the states $|2\rangle$ and $|4\rangle$ are very small, the contribution of ρ_{42} to the third-order susceptibility is not small, as we will see in next section, therefore neglecting the contribution of ρ_{42} to the third-order susceptibility is incorrect [15]. To analyze the enhanced optical nonlinearity of the EIT medium, we use a numerical method, Gaussian elimination, to solve Eqs. (2)-(10) in the steady state and then extract the first-order and the third-order susceptibilities via the relation (12).

III. NUMERICAL COMPARISON OF FOUR-LEVEL AND THREE-LEVEL SYSTEMS

In this section, we numerically compare a four-level EIT system with a three-level EIT system. The three-level system we consider is in fact a special case of the present four-level one. When the atomic transition frequency difference $\omega_{31} - \omega_{42}$ is very large, if the probe frequency ω_p is close to the atomic transition frequency ω_{31} , it will be far detuned from the other atomic transition frequency ω_{42} . In this case, any effect from the state $|4\rangle$ is

negligible, and the four-level system can be approximated as a three-level system with similar parameters. As the three-level system is actually a subsystem of the four-level system, the comparison with the three-level system is not only to show the advantage of the four-level system in enhancing Kerr nonlinearity, but also to show the contribution of the three-level subsystem, i.e., the states $|1\rangle$, $|2\rangle$ and $|3\rangle$, to the third-order susceptibility in the four-level system.

We do the comparison first in terms of third-order susceptibility $\chi^{(3)}$, and then in terms of the ratio between the third-order susceptibility and the first-order susceptibility, i.e., $\chi^{(3)}/\text{Im}\chi^{(1)}$. In the first comparison, we show that there are three major contributions of light shifts of the ground states to $\chi^{(3)}$ in the four-level system: one of them is actually produced within the three-level subsystem, and other two are specific to the four-level system. In particular, we show that there is quantum interference, which does not exist in the four-level system with frequency-non-degenerate probes [6], amongst the three contributions due to atomic coherence. As a result, one can achieve not only larger third-order susceptibility in the four-level system than in the three-level system, but also a control of the ratio between its real and imaginary part. Then in the final part of the section, we consider the finite dephasing rate between the ground states, and further show the advantage of the four-level system in effectively enhancing the third-order nonlinear susceptibility with this new criterion.

A. Analysis in terms of $\chi^{(3)}$

First, following the idea described in the beginning of this section, we let $\omega_{31} - \omega_{42} = -10^5\gamma$ and the four-level system becomes effectively a three-level system. Any contribution of the state $|4\rangle$ to the susceptibility is negligible, so the third-order susceptibility $\chi^{(3)}$, as shown by the dashed lines in Fig. 2 (a) and (b), only originates from the three states $|1\rangle$, $|2\rangle$ and $|3\rangle$, through the off-diagonal density matrix element ρ_{31} . Its real part has already been demonstrated to be much larger than that of the resonantly enhanced susceptibility without the coupling field at a finite detuning [14]. Here we can understand the unusually large magnitude of $\text{Re}\chi^{(3)}$ in a similar way to Ref. [8]: the presence of the weak probe field between the states $|1\rangle$ and $|3\rangle$ causes an energy shift of the state $|2\rangle$, which results in an effective shift of the linear susceptibility $\chi^{(1)}$ curve (see Fig. 2 (c)). However, here there is

an important difference from Ref. [8]: these shifts of the curves are not horizontal shifts along the frequency axis, but changes of the gradients of the curves. For $\text{Re}\chi^{(1)}$, the gradient variation is equivalent to a small rotation of the solid curve around the zero detuning. Then we can understand that although $\text{Re}\chi^{(3)}$ in the situation of EIT is much larger than the resonantly enhanced $\text{Re}\chi^{(3)}$ without the coupling field at a finite detuning, the magnitudes of $\text{Re}\chi^{(3)}$ and $\text{Im}\chi^{(3)}$ also become zero at the zero detuning, as shown in Fig. 2 (a) and (b). Thus the light shift within the three-level subsystem produces a contribution to the third-order susceptibility in the four-level system, and the contribution becomes important when the probe detuning is finite.

Next, let us consider the solo contribution of ρ_{31} to $\chi^{(3)}$ at a small atomic transition frequency difference $\omega_{31} - \omega_{42}$ plotted by the thin solid lines and the thin dot-dashed lines in Fig. 2 (a) and (b). We can find that although both the thin solid curves and the thin dot-dashed curves keep some resemblance of the dashed curves of the three-level system, the magnitudes of some parts of the curves are significantly larger than those of the three-level system at the same frequency. These variations indicate that the presence of the state $|4\rangle$ has important influence on $\chi^{(3)}$ through ρ_{31} . We can understand this effect in the same way as Ref. [6, 8]: the presence of the weak probe field between the states $|2\rangle$ and $|4\rangle$ leads to another energy shift of the state $|2\rangle$, which results in another effective shift of the linear susceptibility $\chi^{(1)}$, i.e., the curves experience additional shifts besides the gradient shifts produced within the three-level subsystem. For the real part of the susceptibility, the shift is mainly along the frequency axis when the atomic transition frequency difference $\omega_{31} - \omega_{42} \neq 0$. Thus the shift results in a finite value of $\text{Re}\chi^{(3)}$ at the center of the transparency window.

Next, following Eq. (12), we include the contribution of ρ_{42} in the calculation of $\chi^{(3)}$, as shown by the thick solid curves and thick dot-dashed curves in Fig. 2 (a) and (b). In comparison with the corresponding thin solid curves and thin dot-dashed curves, we can find that both $\text{Re}\chi^{(3)}$ and $\text{Im}\chi^{(3)}$ are drastically changed once again. In particular, $\text{Im}\chi^{(3)}$ is twice its previous value at zero detuning when $\omega_{31} = \omega_{42}$, as shown by the two solid lines in Fig. 2 (b). This indicates that the contribution of ρ_{42} to $\chi^{(3)}$ is not small, and neglecting its contribution as in Ref. [15] does not give us correct values of $\chi^{(3)}$. We can see that the shift results in another increase of the magnitude of $\text{Re}\chi^{(3)}$ at the center of the transparency window when the atomic transition frequency difference $\omega_{31} - \omega_{42} \neq 0$. Similarly, the energy shift of the state $|2\rangle$ due to the interaction of the weak probe field with the states $|1\rangle$ and

$|3\rangle$ leads to another effective shift of $\chi^{(1)}$ through ρ_{42} .

So far we have found three major contributions of light shifts to the third-order susceptibility in the four-level EIT system. However, the most important feature is that there is quantum interference amongst the three contributions because of the existence of the atomic coherence among the atomic levels. The linear superposition of ρ_{31} and ρ_{42} in Eq. (12) shows explicitly that the interference can occur. Through comparison of the curves of $\chi^{(3)}$ for different contributions in Fig. 2 (a) and (b), we can also discern the variation of the susceptibility due to the interference: the magnitude of $\chi^{(3)}$ may be much increased at certain detuning due to constructive interference, but much reduced at another detuning due to destructive interference. For example, for $\Delta_{13} \approx 0.25\gamma$, the magnitude of $\text{Re}\chi^{(3)}$, plotted by the thick dot-dashed curve in Fig. 2 (a), is increased in comparison with the thin dot-dashed curve and the dashed curve at the same frequency due to constructive interference; however, the magnitude of $\text{Im}\chi^{(3)}$ vanishes at the same detuning due to destructive interference, as shown in Fig. 2 (b). In the four-level system with frequency-non-degenerate probes, there is no such quantum interference effect [6]. This quantum interference process is a unique feature of the four-level system with degenerate probes that we study in this paper. By using this quantum interference we can, not only enhance $\chi^{(3)}$ in the four-level system more than that in the three-level system, but also control the ratio between $\text{Re}\chi^{(3)}$ and $\text{Im}\chi^{(3)}$, as shown in Fig. 3. Comparing the thin curves and the corresponding thick curves, we find that a small probe detuning can produce some zero points for $\text{Im}\chi^{(3)}$ and change the ratio dramatically. If, for example, the four levels are magnetic sub-levels in experiments, one can use a magnetic field to control the atomic transition frequency difference $\omega_{31} - \omega_{42}$ and simultaneously set the probe detuning Δ_{31} to achieve expected ratios. Undoubtedly, such control of the nonlinear susceptibility will be very useful in a practical design of various optical devices.

B. Analysis in terms of $\chi^{(3)}/\text{Im}\chi^{(1)}$

Because the magnitude of a nonlinear effect per unit length becomes very small at very low light intensities, such as when there are few photons per atomic cross section, propagating light beams for a long distance in a nonlinear medium is usually a good way to magnify the nonlinear effect. However, the distance that light beams can propagate is limited by

the linear absorption of the medium, which cannot be zero even under the conditions of EIT because normally γ_{21} is not zero. Thus, the ratio between the nonlinear coefficient and the linear absorption of the medium is the real criterion for the effectiveness of the enhancement of the nonlinear coefficient. We therefore calculate the ratio between the third-order susceptibility $\chi^{(3)}$ and the imaginary part of the first-order susceptibility $\chi^{(1)}$:

$$\lambda = \chi^{(3)}/\text{Im}\chi^{(1)} \quad (13)$$

The results for the four-level system and the three-level system are shown in Figs. 4(a), (b), (c), and (d). In order to determine the positions of the peaks of λ relative to the transparency window, we also depict $\text{Im}\chi^{(1)}$ in Fig. 4(e).

We find that for the four-level system with a small atomic transition frequency difference $\omega_{31} - \omega_{42} = -\gamma$, the position of the largest peak (along the detuning axis) of $\text{Re}\lambda$ (or $\text{Im}\lambda$) is always close to the center of the transparency window independent of the value of the Rabi frequency Ω_{23} , as shown in Figs. 4(a) and (b). In contrast, the three-level system can only produce very small peaks (along the detuning axis) of $\text{Re}\lambda$ at the central part of the transparency window, as shown in Figs. 4(c) and (d). The largest peaks (along the detuning axis) of $\text{Re}\lambda$ (or $-\text{Im}\lambda$) of the three-level system are not in the central region but very close to the two edges of the transparency window, and move away from the center when the transparency window becomes wider, as indicated by the arrows in Figs. 4(c) and (d) — Wang et al. have already demonstrated this phenomenon in their recent experiments [17]. Because the magnitude of $\text{Im}\chi^{(1)}$ at the edges is much larger than at the center [see Fig. 4 (e)], the magnitudes of the largest peaks of λ of the three-level system are much smaller than those of the central peaks of λ of the four-level system as seen in Figs. 4(a) and (b). In this calculation, we assume the dephasing rate $\gamma_{21} = 0.01\gamma$. In this case the largest peak for the three-level system is more than one order smaller than the largest peak for the four-level system.

From the above comparison in terms of λ , we further confirm that the third-order susceptibility $\chi^{(3)}$ is indeed more effectively enhanced in the four-level system, and therefore the four-level system has an advantage for the realization of many quantum nonlinear optics phenomena. However, this conclusion does not mean the contribution of the three-level subsystem to the effectively enhanced λ is negligible. In the next section, we will show the important influence of the quantum interference amongst the three contributions of light

shifts to $\chi^{(3)}$ on the largest peak of λ at a finite probe detuning when the transparency window becomes wider.

IV. BEHAVIOR OF THE LARGEST PEAK OF λ OF THE FOUR-LEVEL SYSTEM

In this section, we consider the detailed behavior of the largest peak of λ of the four-level system with a small atomic transition frequency difference $\omega_{31} - \omega_{42}$ and a finite value of the dephasing rate γ_{21} . Because the dephasing rate γ_{21} is always finite in reality [10, 11], the absorption described by $\text{Im}\chi^{(1)}$ is not zero when $\Delta_{13} = 0\gamma$, and λ is not divergent at this detuning. Thus, it is important in an implementation of the four-level scheme to determine under what condition the most effectively enhanced nonlinear susceptibility occurs under a finite dephasing rate γ_{21} . In Fig. 4 (b), we can easily discern that the value of the largest peak (along the detuning axis) of $\text{Im}\lambda$ increases when the coupling Rabi frequency Ω_{23} increases. By checking more carefully, we find that not only the value of the peak of λ but also the position of the peak depends on the coupling Rabi frequency. This is depicted in Fig. 5.

Fig. 5(a) shows the dependence of the value of the largest peak (along the detuning axis) of $\text{Im}\lambda$, i.e., $(\text{Im}\lambda)_{peak}$, on the Rabi frequency, Ω_{23} , and the atomic transition frequency difference $\omega_{31} - \omega_{42}$. In this calculation, we assume the dephasing rate $\gamma_{21} = 0.01\gamma$. We find that as the coupling Rabi frequency, Ω_{23} , increases, $(\text{Im}\lambda)_{peak}$ (for a fixed value of $\omega_{31} - \omega_{42}$) has a relatively small value at first, increases very rapidly, and then saturates to a relatively large value. For a fixed small value of Ω_{23}/γ , $(\text{Im}\lambda)_{peak}$ decreases monotonically as $(\omega_{31} - \omega_{42})/\gamma$ decreases from 0 to -3 . However, the saturation values for different values of $\omega_{31} - \omega_{42}$ always appear to be the same, and they are always larger than $(\text{Im}\lambda)_{peak}$ at small Ω_{23}/γ . Although the value of the largest peak of $\text{Re}\lambda$, $(\text{Re}\lambda)_{peak}$, is not a monotonic function of $(\omega_{31} - \omega_{42})/\gamma$ at small Ω_{23}/γ , its behavior is quite similar to that of $(\text{Im}\lambda)_{peak}$: as the coupling Rabi frequency Ω_{23} increases, $(\text{Re}\lambda)_{peak}$ always saturates at the same value, which is larger than its value at small Ω_{23}/γ in most cases, as shown in Fig. 5(c). The behavior of the largest peaks of $\text{Re}\lambda$ and $\text{Im}\lambda$ indicate that if the most effectively enhanced nonlinear susceptibility is desired under a finite γ_{21} , then the coupling Rabi frequency Ω_{23} should be set as large as possible. This is especially true when the magnitude of the atomic

transition frequency difference is not small.

Next, from Fig. 5(b) [or (d)], we find that for a fixed value of $(\omega_{31} - \omega_{42})/\gamma$, when $(\text{Im}\lambda)_{peak}$ (or $(\text{Re}\lambda)_{peak}$) increases and saturates, the detuning $(\Delta_{13})_{peak}$, at which the largest peak occurs, also shifts asymptotically from $(\Delta_{13})_{peak} = 0$ to another finite value. The asymptotic value of the detuning is always equal to $-(\omega_{31} - \omega_{42})/2$, as shown in Fig. 5(b). This value exactly corresponds to the frequency of the probe light being resonant with the two-photon transitions between states $|1\rangle \leftrightarrow |4\rangle$, i.e., $2\omega_p = \omega_{31} + \omega_{42}$. The asymptotic value of the detuning at which the largest peak of $\text{Re}\lambda$ occurs is always a half line width, $\gamma/2$, away from that of the largest peak of $\text{Im}\lambda$ for the same $(\omega_{31} - \omega_{42})/\gamma$, as shown in Fig. 5(d). This behavior of the largest peaks of $\text{Re}\lambda$ and $\text{Im}\lambda$ indicates that while the transparency window becomes wider, the constructive quantum interference amongst the three contributions of light shifts becomes more important, and the peak of λ therefore shifts to a nonzero probe detuning. Thus if a most effectively enhanced nonlinear susceptibility is desired under a finite γ_{21} , the detuning of the probe light should be set close to the asymptotic values found in the above analysis. This is especially true when the magnitude of the atomic transition frequency difference is not very small. Even if a certain ratio between $\text{Re}\chi^{(3)}$ and $\text{Im}\chi^{(3)}$ is required, the asymptotic values shown above will be important for determining the optimum detuning setting. Setting the detuning to zero, i.e., the center of the transparency window, might not be the best choice.

Additionally, an interesting case occurs when $\omega_{31} - \omega_{42} = -\gamma$ (or 0γ). In this case, $(\text{Re}\lambda)_{peak}$ (or $(\text{Im}\lambda)_{peak}$) reaches its saturation value for very small values of Ω_{23} . This means that the enhancement of the nonlinear susceptibility can occur at very low coupling light intensity.

In the calculations in Fig. 4 and Fig. 5, we assumed the dephasing rate of the ground states is $\gamma_{21} = 0.01\gamma$. More generally, we can calculate the dependence of the saturation values of the largest peaks of λ on the dephasing rate γ_{21} , as shown in Fig. 6. If the dephasing rate γ_{21} is much smaller than the decay rate γ of the upper levels, then the four-level system can enhance the nonlinear susceptibility more effectively, as indicated by λ . This means that in order to employ the four-level system to more effectively enhance the nonlinearity, one needs to reduce the dephasing rate of the ground states as much as possible.

The analysis of the behavior of the largest peak of λ also demonstrates the importance of the quantum interference amongst the three contributions of light shifts to $\chi^{(3)}$ when the

transparency window is very wide. To implement the four-level system with a finite γ_{21} to more effectively enhance the nonlinear susceptibility, the coupling Rabi frequency Ω_{23} should be set as large as possible and simultaneously the detuning of the probe light should be set as close as possible to the asymptotic values found in the above analysis. This is particularly important when the magnitude of the atomic transition frequency difference is not so small. This conclusion is very different from the proposal in Ref. [15] due to the fact that in that work only the very special case when the dephasing rate vanishes, $\gamma_{21} = 0$, was considered.

V. CONCLUSION

We have studied in detail the third-order susceptibility for self-action of a four-level system, including the dephasing between the two ground states, under the condition of EIT by numerically solving the steady-state equations for the atomic density matrix. Through comparison of the four-level system with a three-level system with the same characteristic parameters, we discerned three major contributions from light shifts to the third-order susceptibility in the four-level system. In particular, we found that quantum interference amongst the three contributions, which does not exist in the four-level system with frequency-non-degenerate probes [6], can not only enhance the third-order susceptibility more effectively in the four-level system than in the three-level system, but also make the ratio between its real part and imaginary part controllable. This unique feature means the four-level system has certain advantages for the realization of many quantum nonlinear optics phenomena. In implementing this scheme, it is important to note that in general the most effective enhancement of the nonlinear susceptibility does not occur exactly at the center of the transparency window. Instead, due to the constructive quantum interference, and a finite dephasing rate between the two ground states, the most effective enhancement occurs at an offset that is determined by the atomic transition frequency difference and the coupling Rabi frequency.

-
- [1] R. Y. Chiao and I. H. Deutsch, Phys. Rev. Lett. **67**, 1399 (1991); I. H. Deutsch and Raymond Y. Chiao, Phys. Rev. Lett. **69**, 3627 (1992).

- [2] P. D. Drummond, R. M. Shelby, S. R. Friberg, Y. Yamamoto, *Nature (London)* **365**, 307 (1993); M. J. Werner, *Phys. Rev. Lett.* **81**, 4132 (1998).
- [3] S. E. Harris, *Phys. Today* **50**, 36 (1997); E. Arimondo, in *Progress in Optics XXXV*, edited by E. Wolf (Elsevier, Amsterdam, 1996), p. 257.
- [4] S. E. Harris, J. E. Field, and A. Imamoglu, *Phys. Rev. Lett.* **64**, 1107 (1990).
- [5] K. Hakuta, L. Marmet, and B. P. Stoicheff, *Phys. Rev. Lett.* **66**, 596 (1991).
- [6] H. Schmidt and A. Imamoglu, *Opt. Lett.* **21**, 1936 (1996).
- [7] S. E. Harris and Y. Yamamoto, *Phys. Rev. Lett.* **81**, 3611 (1998); S. E. Harris and L. Hau, *Phys. Rev. Lett.* **82**, 4611 (1999).
- [8] M. D. Lukin and A. Imamoglu, *Phys. Rev. Lett.* **84**, 1419 (2000). M. Fleischhauer and M. D. Lukin, *Phys. Rev. Lett.* **84**, 5094 (2000); M. D. Lukin, A. Imamoglu, *Nature* **413**, 273 (2001).
- [9] A. Imamoglu, H. Schmidt, G. Woods, and M. Deutsch, *Phys. Rev. Lett.* **79**, 1467 (1997); M. D. Lukin, C. S. F. Yelin, and M. Fleischhauer, *Phys. Rev. Lett.* **84**, 4232 (2000); M. D. Lukin et al., *Phys. Rev. E. Lett.* **81**, 2675 (1998);
- [10] M. Xiao, Y. Li, S. Jin, and J. Gea-Banacloche, *Phys. Rev. Lett.* **74**, 666 (1995); L. V. Hau, S. E. Harris, Z. Dutton, and C. H. Behroozi, *Nature (London)* **397**, 594 (1999); M. M. Kash, V. A. Sautenkov, A. S. Zibrov, L. Hollberg, G. R. Welch, M. D. Lukin, Y. Rostovtsev, F. S. Fry and M. O. Scully, *Phys. Rev. Lett.* **82**, 5229 (1999); D. Budker, D. F. Kimball, H. S. M. Rochester, and V. V. Yashchuk, *Phys. Rev. I. Lett.* **83**, 1767 (1999).
- [11] A. J. Merriam et al., *Phys. Rev. Lett.* **84**, 5308 (2000); M. Jain, H. Xia, G. Y. Yin, A. J. Merriam, and S. H. Harris, *Phys. Rev. Lett.* **77**, 4326 (1996); P. R. Hemmer et al., *Opt. Lett.* **20**, 982 (1995); B. Lu, W. H. Burkett, and M. Xiao, *Opt. Lett.* **23**, 804 (1998); Y. Li and M. Xiao, *Opt. Lett.* **21**, 1064 (1996).
- [12] R. R. Moseley et al., *Phys. Rev. Lett.* **74**, 670 (1995); M. Jain, A. J. Merriam, A. J. Kasapi, G. Y. Yin, and S. E. Harris, *Phys. Rev. Lett.* **75**, 4385 (1995).
- [13] M. Mitsunaga, M. Yamashita and H. Inoue, *Phys. Rev. A* **62**, 013817 (2000).
- [14] H. Wang, D. Goorskey, and M. Xiao, *Phys. Rev. Lett.* **87**, 073601 (2001); H. Wang, D. Goorskey, and M. Xiao, *Phys. Rev. A* **65** 011801 (2002); H. Wang, D. Goorskey, and M. Xiao, *Phys. Rev. A* **65**, 051802 (2002).
- [15] A. Imamoglu, H. Schmidt, G. Woods, and M. Deutsch, *Phys. Rev. Lett.* **79**, 1467 (1997).
- [16] P. Meystre, M. Sargent III, *Elements of Quantum Optics* (Springer-Verlag, Berlin, 1999).

[17] H. Wang, D. Goorskey, and M. Xiao, *Opt. Lett.* **27**, 258 (2002).

VI. FIGURE CAPTIONS

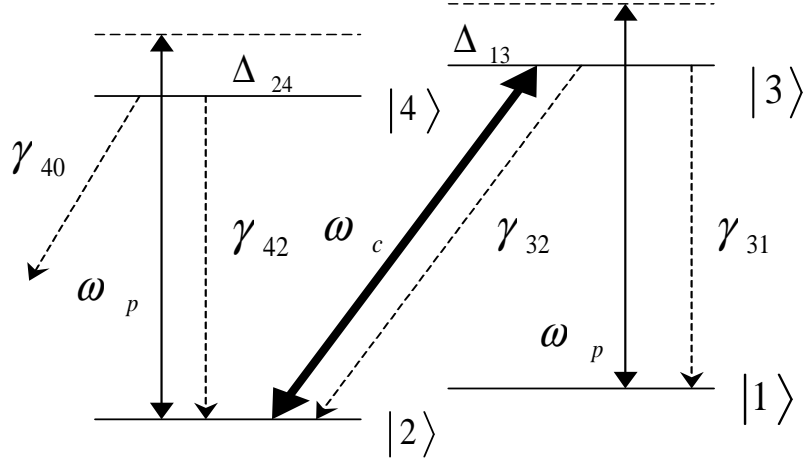


FIG. 1: Energy levels and optical couplings of the four-level atomic system. ω_c is the angular frequency of the coupling light, and ω_p the angular frequency of the degenerate probe light. Direct electric-dipole transition between two ground states, $|1\rangle$ and $|2\rangle$, is assumed to be forbidden. γ_{31} , γ_{32} , γ_{42} are decay rates from excited states to the ground states. γ_{40} is the decay rate of the state $|4\rangle$ to states other than these four states. Δ_{13} and Δ_{24} are detuning frequencies of the degenerate probe light.

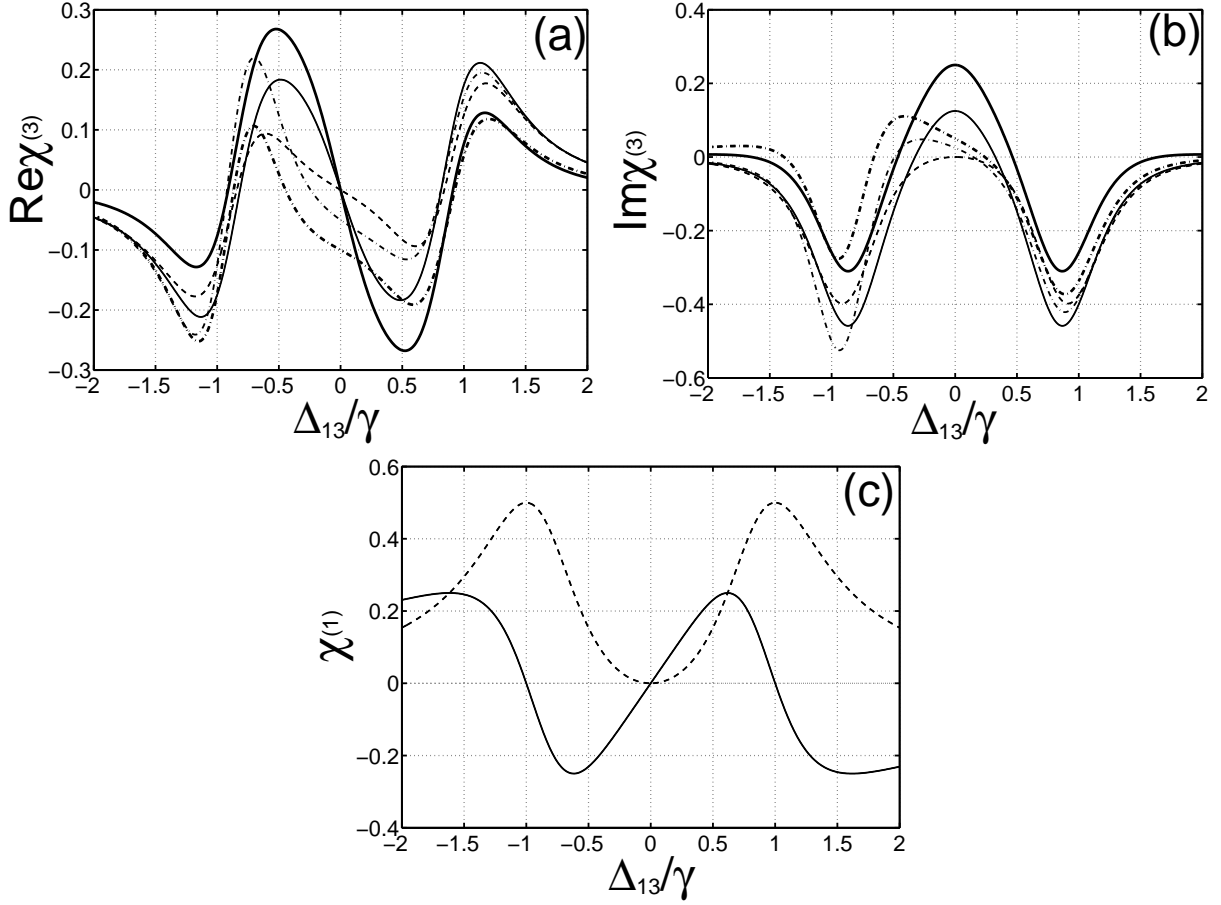


FIG. 2: Probe susceptibilities vs the probe detuning frequency. (a) and (b) show the real and imaginary parts of the third-order susceptibility $\chi^{(3)}$ for the four-level system in three cases: $\omega_{31} - \omega_{42} = -10^5\gamma$ (dashed lines, an approximation to a three level system), $\omega_{31} = \omega_{42}$ (thick solid lines) and $\omega_{31} - \omega_{42} = 2\gamma$ (thick dot-dashed lines). $\chi^{(3)}$ is in units of $2n\mu^4/(\varepsilon_0\hbar^3\gamma^3)$. In addition, they also show the solo contribution of ρ_{31} to $\chi^{(3)}$ in the second case (thin solid lines) and the third case (thin dot-dashed lines). (c) shows the transparency window: the real part (solid line) and imaginary part (dashed line) of the first-order susceptibility $\chi^{(1)}$ both become zero at $\Delta_{13} = 0\gamma$. $\chi^{(1)}$ is in units of $2n\mu^2/(\varepsilon_0\hbar\gamma)$. In the calculation, $\gamma_{21} = 0\gamma$ and $\Omega_{23} = 2\gamma$.

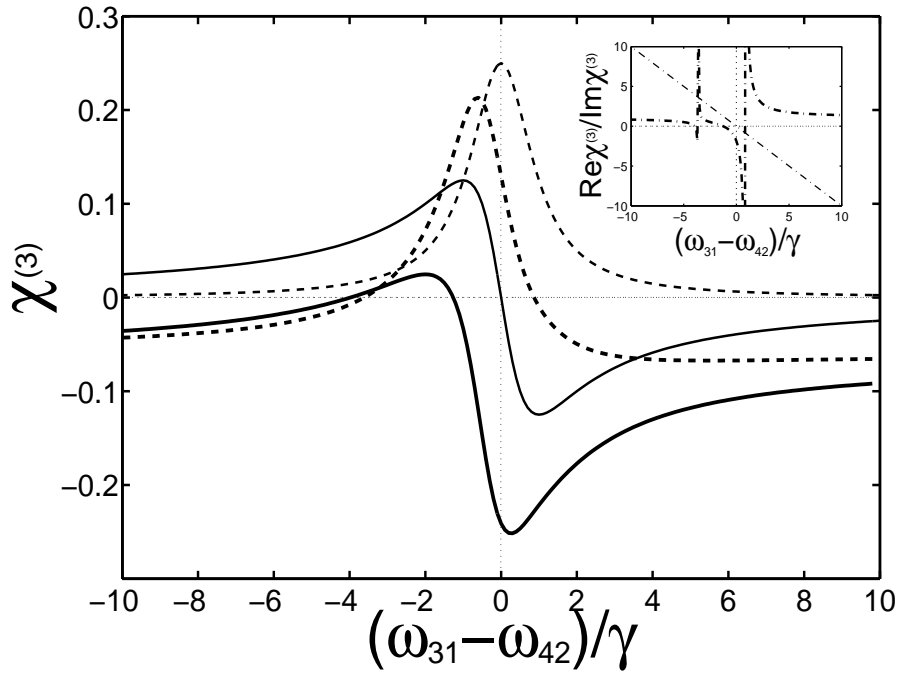


FIG. 3: The third-order susceptibility $\chi^{(3)}$ vs the atomic transition frequency difference $\omega_{31} - \omega_{42}$ in the four-level system for two kinds of probe detunings Δ_{13} . The real and imaginary parts of $\chi^{(3)}$ in units of $2n\mu^4/(\epsilon_0\hbar^3\gamma^3)$ are represented by the solid line and the dashed line, respectively. The inset shows the ratio between the real part and the imaginary part of $\chi^{(3)}$ as a function of $\omega_{31} - \omega_{42}$. In the calculation, $\Delta_{24} = \omega_{31} - \omega_{42}$, $\Omega_{23} = 2\gamma$ and $\Delta_{13} = 0\gamma$ (thin lines) or 0.4γ (thick lines).

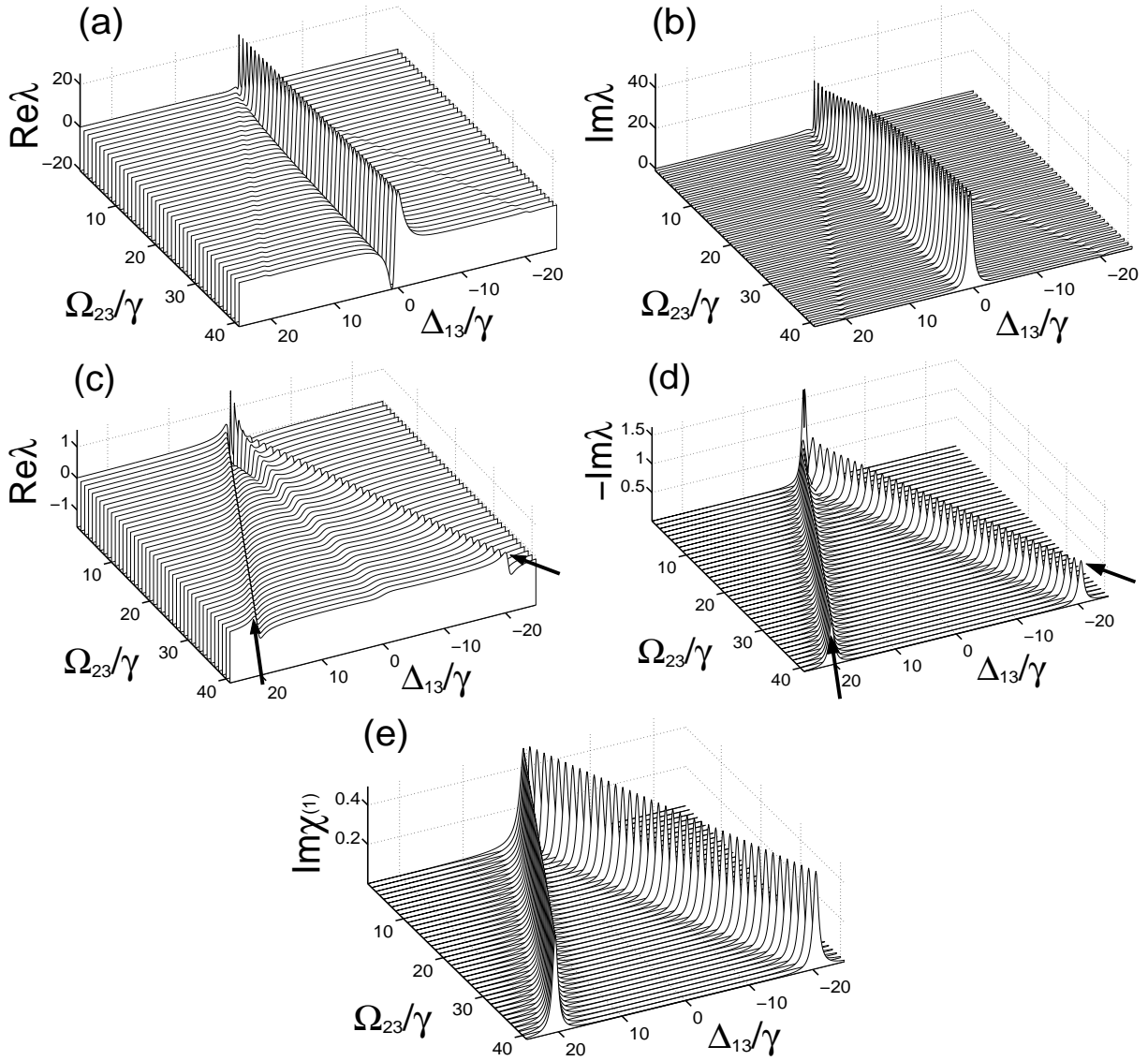


FIG. 4: Ratio λ vs the probe detuning Δ_{13} and the Rabi frequency Ω_{23} . (a) and (b) show the ratio for the four-level system with $\omega_{31} - \omega_{42} = -\gamma$. (c) and (d) show the ratio for the three-level system, i.e., the approximation of the four-level system with $\omega_{31} - \omega_{42} = -10^5\gamma$. (e) shows the imaginary part of the first-order susceptibility $\chi^{(1)}$. The ratio λ is in units of $\mu^2/(\hbar\gamma)^2$, and the linear susceptibility is in units of $2n\mu^2/(\epsilon_0\hbar\gamma)$. In this calculation, $\gamma_{21} = 0.01\gamma$.

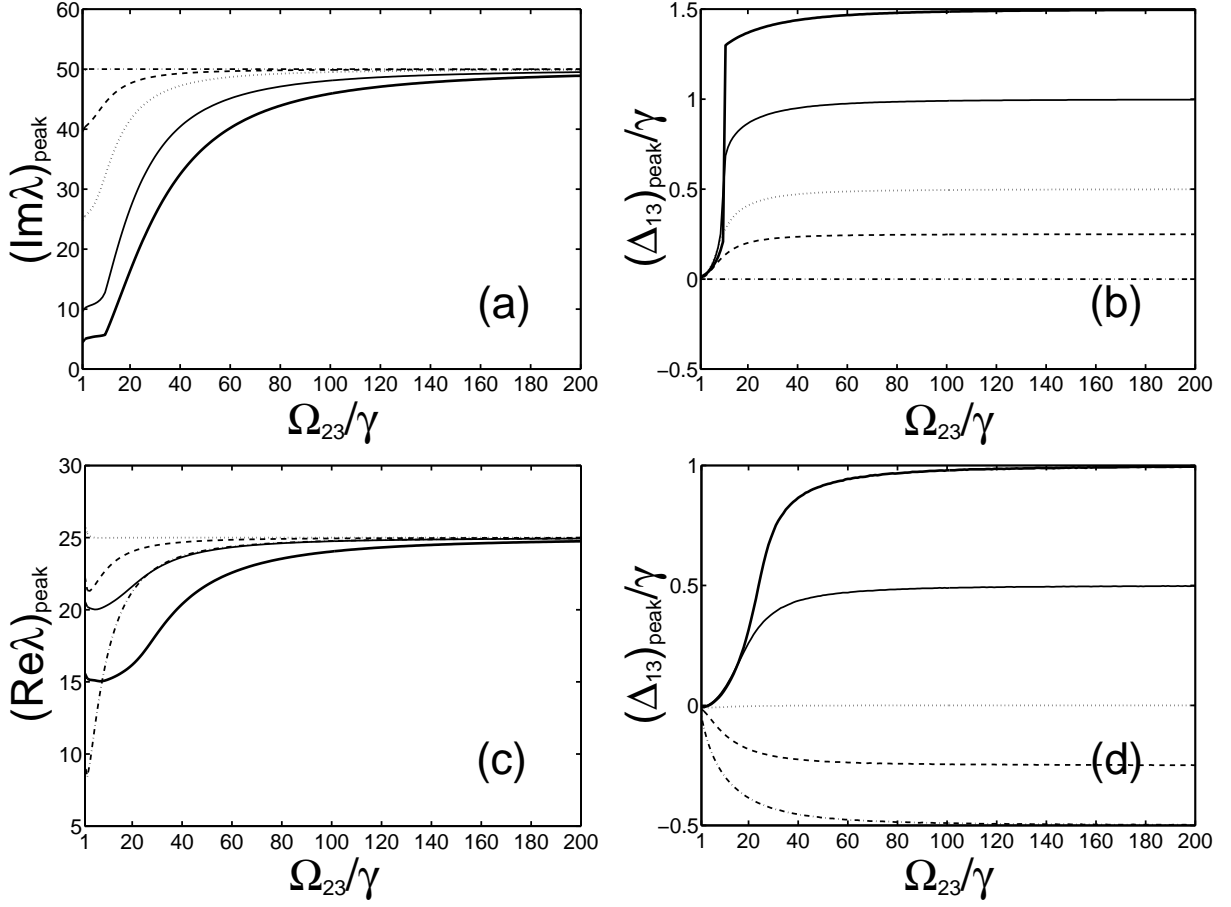


FIG. 5: Value and detuning of the largest peak of λ vs the Rabi frequency Ω_{23} and the atomic transition frequency difference $\omega_{31} - \omega_{42}$. (a) and (b) are for the imaginary part of λ . (c) and (d) are for the real part of λ . The curves for $(\omega_{31} - \omega_{42})/\gamma = 0, -0.5, -1, -2, -3$ are plotted by dot-dashed lines, dashed lines, dotted lines, thin solid lines and thick solid lines, respectively. The ratio λ is in units of $\mu^2/(\hbar\gamma)^2$. In this calculation, the dephasing rate $\gamma_{21} = 0.01\gamma$.

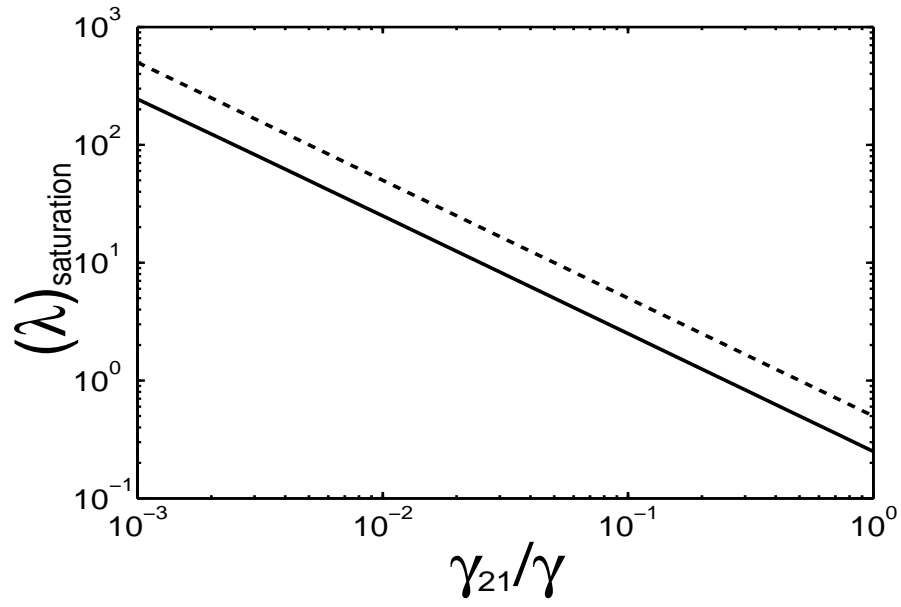


FIG. 6: Saturation value of the largest peak of λ vs the dephasing rate γ_{21} . The ratio λ is in units of $\mu^2/(\hbar\gamma)^2$. The solid line is for the real part of λ , and the dashed line for the imaginary part of λ .